electronics

Article

Current-Mode First-Order Versatile Filter Using Translinear Current Conveyors with Controlled Current Gain

Montree Kumngern [1], Wirote Jongchanachavawat [2], Punnavich Phatsornsiri [3], Natapong Wongprommoon [4], Fabian Khateb [5,6,7,*] and Tomasz Kulej [8]

1. Department of Telecommunications Engineering, School of Engineering, King Mongkut's Institute of Technology Ladkrabang, Bangkok 10520, Thailand; montree.ku@kmitl.ac.th
2. Faculty of Engineering and Industrial, Phetchaburi Rajabhat University, Phetchaburi 76000, Thailand; wirote.jon@mail.pbru.ac.th
3. Faculty of Engineering, Pathumwan Institute of Technology, Bangkok 10330, Thailand; ppunnavich@pit.ac.th
4. Faculty of Engineering and Industrial Technology, Silpakorn University, Nakhon Pathom 73000, Thailand; w.natapong@gmail.com
5. Department of Microelectronics, Brno University of Technology, Technická 10, 601 90 Brno, Czech Republic
6. Faculty of Biomedical Engineering, Czech Technical University in Prague, Nám. Sítná 3105, 272 01 Kladno, Czech Republic
7. Department of Electrical Engineering, Brno University of Defence, Kounicova 65, 662 10 Brno, Czech Republic
8. Department of Electrical Engineering, Czestochowa University of Technology, 42-201 Czestochowa, Poland; kulej@el.pcz.czest.pl

* Correspondence: khateb@vutbr.cz

Abstract: This paper offers a new current-mode first-order versatile filter employing two translinear current conveyors with controlled current gain and one grounded capacitor. The proposed filter offers the following features: realization of first-order transfer functions of low-pass, high-pass, and all-pass current responses from single topology, availability of non-inverting and inverting transfer functions for all current responses, electronic control of current gain for all current responses, no requirement of component-matching conditions for realizing all current responses, low-input impedance and high-output impedance which are required for current-mode circuits, and electronic control of the pole frequency for all current responses. The proposed first-order versatile filter is used to realize a quadrature sinusoidal oscillator to confirm the advantage of the new topology. To confirm the functionality and workability of new circuits, the proposed circuit and its application are simulated by the SPICE program using transistor model process parameters NR100N (NPN) and PR100N (PNP) of bipolar arrays ALA400-CBIC-R from AT&T.

Keywords: current-mode circuit; first-order filter; second-generation current conveyor; translinear current conveyor

check for updates

Citation: Kumngern, M.; Jongchanachavawat, W.; Phatsornsiri, P.; Wongprommoon, N.; Khateb, F.; Kulej, T. Current-Mode First-Order Versatile Filter Using Translinear Current Conveyors with Controlled Current Gain. *Electronics* **2023**, *12*, 2828. https://doi.org/10.3390/electronics12132828

Academic Editors: Gaetano Palumbo and Esteban Tlelo-Cuautle

Received: 16 May 2023
Revised: 15 June 2023
Accepted: 23 June 2023
Published: 26 June 2023

1. Introduction

Second-generation current conveyor (CCII) has been widely accepted to realize current-mode filters because the CCII offers better signal bandwidth, linearity, and dynamic range performances compared with operational amplifier (op-amp) based [1,2]. First-order filters are important sub-circuits for applications such as quadrature oscillators [3], multiphase oscillators [4], and high-order filters [5]. Usually, universal first-order filters are the circuits that can realize three filtering functions such as low-pass (LP), high-pass (HP), and all-pass (AP), into a single topology. Several universal first-order filters are available in the open literature [6–34]. It should be noted that the universal first-order filter is an interesting topic for publications because many papers on this topic were published in a few years ago [28–34]. Considering the mode of operations, these first-order filters can be classified as voltage-mode (VM) filters [6–14], current-mode (CM) filters [15–30], and mixed-mode (MM) filters [31–34]. This work is focused on CM filters that should provide low-input and high-output impedances, which is ideal for CM circuits because they can be connected to applications without buffer circuit requirements. Single-input three-output current filters are required because, when a single input signal is used, variant filtering functions can be obtained at the outputs without additional circuitry requirements, such as a current splitter circuit used to split a single currency into multiple currents for multi-input current filters.

Considering CM and MM filters in [15–34], only the circuits in [15,24] can realize six transfer functions into a single topology, namely, both non-inverting and inverting transfer functions of LP, HP, and AP are obtained. However, the current gain of these transfer functions cannot be controlled. The first-order filter that can adjust the current gain of transfer functions has been proposed in [16], but only three transfer functions of LP, HP, and AP filters are obtained. The circuits that offer low-input and high-output impedances have been reported in [15,21,25,26,29], and several filters offer electronic control of the pole frequency [17,25–27,30–32,34]. However, these first-order filters cannot control the gain of transfer functions, and some of these filters offer only three transfer functions LP, HP, and AP filters. The circuits in [16,19,24] use a floating capacitor, which is not ideal for integrated circuits. The circuits in [29,34] require two identical input signals, so an additional current splitter circuit is needed.

Filters that can provide current gains of transfer functions are required because they can be used as a parameter for applications such as the condition of oscillation for oscillator circuits, which will be demonstrated in this paper. In addition, filters that offer the ability to electronically tune the pole frequency can provide advantages in case of easy compensation when the pole frequency deviates due to temperature, power supply, and process variations. Moreover, filters that can tune the pole frequency using a single parameter, such as a single bias current without matching conditions for any parameter during the tuning process, are of interest because they can be easily controlled in practice.

In this paper, a new current-mode current-controlled versatile first-order filter employing two translinear current conveyors with controlled current gain and one grounded capacitor is proposed. The circuit can simultaneously realize non-inverting and inverting transfer functions of LP, HP, and AP current answers with low-input and high-output impedances; hence six transfer functions can be obtained. The current gain and pole frequency of all transfer functions can be electronically controlled. To the best of the authors' knowledge, there is no first-order current filter published in the literature that works similarly to this work. The non-ideal analysis of the proposed filter is further investigated. The HP filter is chosen for application to the quadrature oscillator by incorporating a lossy integrator. The proposed first-order filter and quadrature oscillator are simulated using the SPICE program to validate the theoretical formulations. The paper is organized as follows: Section 2 describes the structure of the second-generation current-controlled current conveyor (CCCII) and the proposed current-mode versatile first-order filter. Section 3 provides the non-ideality analysis for the proposed circuit. Section 4 presents an application of a current-mode quadrature oscillator. The simulation results of the CCCII, the filter, and the oscillator are shown in Section 5. Section 6 concludes the paper.

2. Circuit Description

The second-generation current-controlled current conveyor (CCCII) was first introduced in [35]. Compared with the conventional second-generation current conveyors (CCII) that have three terminals (y-, x-, and z-terminals), CCCII has parasitic resistance R_x at the x-terminal that usually can be controlled by bias current, and its ideal characteristic can be given by

$$\begin{pmatrix} I_y \\ V_x \\ I_z \end{pmatrix} = \begin{pmatrix} 0 & 0 & 0 \\ 1 & R_x & 0 \\ 0 & 1 & 0 \end{pmatrix} = \begin{pmatrix} V_y \\ I_x \\ V_z \end{pmatrix} \tag{1}$$

The y- and z-terminals possess high impedances (infinite for ideal), and the x-terminal has the parasitic resistance R_x.

It should be noted that the CCCII has a unity voltage gain between the y- and x-terminals and a unity current gain between the x- and z-terminals. To increase the performance of CCCII or CCII by controlling the current gain between x- and z-terminals, the CCCII/CCII with controlled current gain has been proposed [36–41]. Thus, a CCCII with controlled current gain has a limited resistance R_x at x-terminal and the current gain between the x- and z-terminals. Therefore, there are two parameters (R_x and current gain) available for user applications in the single CCCII with controlled current gain.

Figure 1 shows the proposed translinear current conveyors with controlled current gain, which was realized using bipolar junction transistors (BJTs). It was modified from [35] by adding current mirrors with adjustable gain (Q_{22}–Q_{25} and Q_{26}–Q_{29}) [2,36].

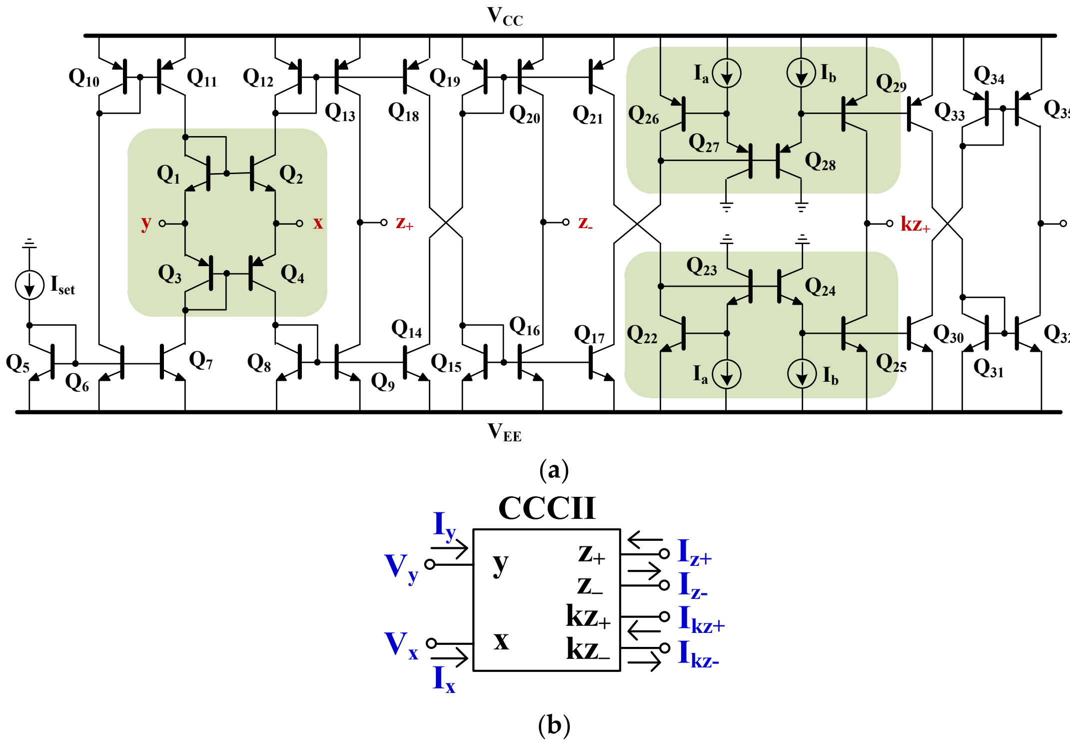

Figure 1. Translinear current conveyors with controlled current gain, (**a**) schematic, (**b**) electrical symbol.

To obtain the required plus and minus current outputs of the translinear current conveyor, adding additional current mirrors and cross-coupled current mirrors [42] are used. Consider a translinear-mixed loop (Q_1 to Q_4) and assume Q_5–Q_8 and Q_{10}–Q_{12} around the loop are identical; the limited resistance R_x at x-terminal can be given by [35]

$$R_x = \frac{V_T}{2I_{set}} \tag{2}$$

where I_{set} is the bias current, and V_T is the thermal voltage (V_T = 25.8 mV at room temperature). It should be noted that the resistance R_x can be controlled by the dc bias current I_{set}.

Consider positive and negative current mirrors with adjustable gain by assuming that Q_{22}–Q_{25} and Q_{26}–Q_{29} are identical; the current gain k of the current conveyor in Figure 1 can be given by [2,36]

$$k = \frac{I_a}{I_b} \tag{3}$$

Thus, the signal current from x- to kz-terminals is amplified by the factor k, which can be given by I_a/I_b ($k = I_a/I_b$). It should be noted that the factor k can be linearly controlled, which can only be obtained using BJT-based CCCII in Figure 1. Therefore, the port characteristics of the translinear current conveyor with controlled current gain in Figure 1 can be expressed by

$$\begin{pmatrix} I_y \\ V_x \\ I_z \\ I_{kz} \end{pmatrix} = \begin{pmatrix} 0 & 0 & 00 \\ 1 & R_x & 00 \\ 0 & \pm 1 & 00 \\ 0 & \pm k & 00 \end{pmatrix} = \begin{pmatrix} V_y \\ I_x \\ V_z \\ V_{kz} \end{pmatrix} \tag{4}$$

The proposed current-mode versatile first-order filter is shown in Figure 2. It consists of two translinear current conveyors with controlled current gains and one grounded capacitor. The use of grounded capacitors is advantageous for integrated circuits because their behavior is less affected by noise and stray capacitance effects compared to circuits using floating capacitors. It should be noted that the input signal is applied to the low-impedance (x-terminal) of CCCII, while the output signals are obtained from the high-impedance (z-terminal) of CCCII. Thus, the proposed filter provides low-input and high-output impedances.

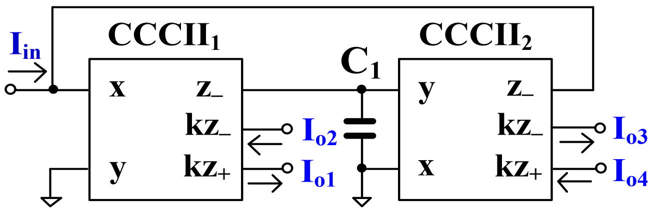

Figure 2. Proposed current-mode versatile first-order filter.

Using (4) and nodal analysis, the current outputs I_{o1}, I_{o2}, I_{o3}, and I_{o4} of the proposed filter in Figure 2 can be given by

$$I_{o1} = -I_{o2} = k_1 \left(\frac{sC_1 R_{x2}}{sC_1 R_{x2} + 1} \right) I_{in} \tag{5}$$

$$I_{o3} = -I_{o4} = k_2 \left(\frac{1}{sC_1 R_{x2} + 1} \right) I_{in} \tag{6}$$

Thus, the proposed filter offers both non-inverting and inverting first-order transfer functions of HP and LP filters. The current gains of the HP and LP filters can be controlled by k_1 and k_2, respectively, where $k_1 = I_{a1}/I_{b1}$, $k_2 = I_{a2}/I_{b2}$, and I_{a1}, I_{a2}, I_{b1}, I_{b2} are the bias currents of the current mirrors with an adjustable gain of the CCCIIs. The non-inverting first-order AP filter (phase lag) can be obtained by connecting I_{o2} and I_{o3} ($I_{o2} + I_{o3}$) and the inverting first-order AP filter (phase lead) can be obtained by connecting I_{o1} and I_{o4} ($I_{o1} + I_{o4}$). Their transfer functions can be expressed by

$$\frac{I_{AP+}}{I_{in}} = \frac{I_{o2} + I_{o3}}{I_{in}} = k\frac{1 - sC_1 R_{x2}}{1 + sC_1 R_{x2}} = -k\frac{sC_1 R_{x2} - 1}{sC_1 R_{x2} + 1} \tag{7}$$

$$\frac{I_{AP-}}{I_{in}} = \frac{I_{o1} + I_{o4}}{I_{in}} = k\frac{sC_1 R_{x2} - 1}{sC_1 R_{x2} + 1} \tag{8}$$

where $k_1 = k_2 = k$. Thus, the current gains of the AP filters can be controlled by k ($k = I_{a1}/I_{b1} = I_{a2}/I_{b2}$).

Equations (5)–(8) confirm that that the proposed filter offers six transfer functions of LP, HP, and AP filters from a single topology.

The pole frequency of all filters can be calculated as

$$\omega_o = \frac{1}{sC_1 R_{x2}} \tag{9}$$

Thus, the pole frequency can be electronically controlled by R_{x2} through the dc bias current I_{set2} of the $CCCII_2$. It should be noted that the pole frequency can be adjusted by the single bias current I_{set2} without matching conditions for any parameter during the tuning process.

3. Non-Ideality Analysis

The relationship of the voltages and currents by taking the non-idealities of the translinear current conveyor with controlled current gain can be described as

$$\begin{pmatrix} I_y \\ V_x \\ I_z \\ I_{kz} \end{pmatrix} = \begin{pmatrix} 0 & 0 & 00 \\ \alpha & R_x & 00 \\ 0 & \pm\beta & 00 \\ 0 & \pm\beta_k k & 00 \end{pmatrix} = \begin{pmatrix} V_y \\ I_x \\ V_z \\ V_{kz} \end{pmatrix} \tag{10}$$

where $\alpha = 1 - \varepsilon_v$ and ε_v ($\varepsilon_v \ll 1$) is the voltage tracking error from y- to x-terminals, $\beta_1 = 1 - \varepsilon_i$ and ε_i ($\varepsilon_i \ll 1$) is the output current tracking error from x- to z-terminals, $\beta_2 = 1 - \varepsilon_{ik}$ and ε_{ik} ($\varepsilon_{ik} \ll 1$) is the output current tracking error from x- to kz-terminals.

The various parasitic elements in the non-ideal CCCII symbol are shown in Figure 3. It shows that the x-terminal illustrates limited parasitic serial resistance R_x, the y-terminal illustrates high-value parasitic resistance R_y in parallel with low-value parasitic capacitance C_y, the z-terminal illustrates high-value parasitic resistance R_z in parallel with low-value parasitic capacitance C_z, and the kz-terminal illustrates high-value parasitic resistance R_{kz} in parallel with low-value parasitic capacitance C_y.

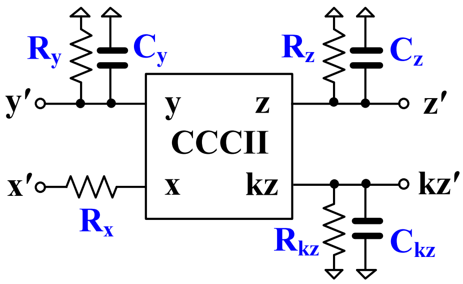

Figure 3. CCCII with its parasitic components.

Using (10) and Figure 3, the current outputs I_{o1}, I_{o2}, I_{o3}, and I_{o4} can be rewritten as

$$I_{o1} = -I_{o2} = \beta_{k1} k_1 \left(\frac{\beta_1 (sC_T R_{x2} + G_T R_{x2})}{(sC_T R_{x2} + G_T R_{x2}) + \beta_1 \beta_2 \alpha_2} \right) I_{in} \tag{11}$$

$$I_{o3} = -I_{o4} = \beta_{k2} k_2 \left(\frac{\beta_1 \beta_2 \alpha_2}{(sC_T R_{x2} + G_T R_{x2}) + \beta_1 \beta_2 \alpha_2} \right) I_{in} \tag{12}$$

The transfer functions of APFs become

$$\frac{I_{AP+}}{I_{in}} = \frac{I_{o2} + I_{o3}}{I_{in}} = -\frac{\beta_1 \beta_{k1} k_1 (sC_T R_{x2} + G_T R_{x2}) - \beta_1 \beta_2 \alpha_2 \beta_{k2} k_2}{(sC_T R_{x2} + G_T R_{x2}) + \beta_1 \beta_2 \alpha_2} \tag{13}$$

$$\frac{I_{AP-}}{I_{in}} = \frac{I_{o1} + I_{o4}}{I_{in}} = \frac{\beta_1 \beta_{k1} k_1 (sC_T R_{x2} + G_T R_{x2}) - \beta_1 \beta_2 \alpha_2 \beta_{k2} k_2}{(sC_T R_{x2} + G_T R_{x2}) + \beta_1 \beta_2 \alpha_2} \tag{14}$$

where $C_T = C_1 + C_{z1} + C_{y2}$, $G_T = (1/R_{z1})//(1/R_{y1})$.

All filters have a pole frequency that can be calculated as

$$\omega_o = \frac{\beta_1 \beta_2 \alpha_2}{sC_T R_{x2} + G_T R_{x2}} \tag{15}$$

It should be noted that the impact of the parasitic capacitances C_{z1} + C_{y2} can be eliminated if the large value of C_1 is used, and the impact of the parasitic resistances $R_{z1}//R_{y1}$ can be eliminated if the low value of R_{x2} is given. However, the voltage and current gains of CCCIIs change the pole frequency.

4. Application to Quadrature Oscillator

Figure 4 shows the application of the proposed versatile filter as a current-mode quadrature oscillator. The current-mode high-pass filter has been selected, and it cascaded with a current-mode lossy integrator. When the circuit is connected as a feedback loop, the characteristic equation of the system can be stated by

$$k_1\left(\frac{sC_1R_{x2}}{sC_1R_{x2}+1}\right)\left(\frac{1}{sC_2R_{x3}+1}\right)=0 \tag{16}$$

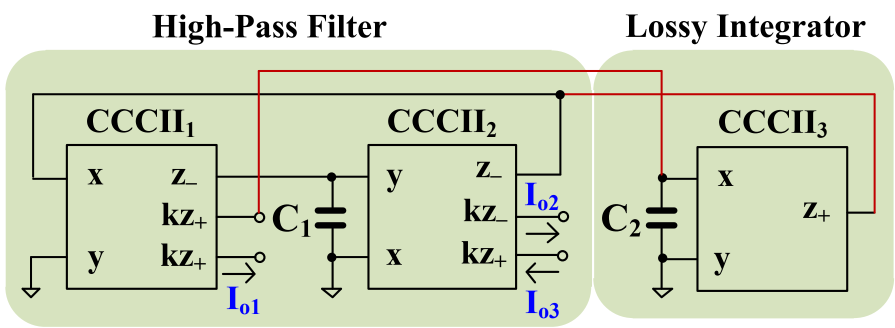

Figure 4. Current-mode quadrature oscillator.

The characteristic equation of the oscillator can be stated by

$$s^2C_1C_2R_{x2}R_{x3}+s(C_1R_{x2}+C_2R_{x3}-k_1C_1R_{x2})+1=0 \tag{17}$$

The system will generate the sinusoidal signal under the condition of oscillation (CO) as

$$k_1=\frac{C_1R_{x2}+C_2R_{x3}}{C_1R_{x2}} \tag{18}$$

Letting $C_1 = C_2$ and $R_{x2} = R_{x3}$, the CO becomes

$$k_1=2 \tag{19}$$

where R_{x2} and R_{x3} are, respectively, the parasitic resistances at x-terminals of $CCCII_2$ and $CCCII_3$, k_1 is the current gain of $CCCII_1$.

The frequency of oscillation (FO) is

$$\omega_o=\frac{1}{\sqrt{C_1C_2R_{x2}R_{x3}}} \tag{20}$$

The CO is controlled by current gain k_1 and the FO is controlled by R_{x2} and R_{x3} ($R_{x2} = R_{x3}$). Thus, the CO and FO can be controlled electronically and independently.

Consider Figure 4, the $CCCII_2$ and C_2 work as a lossless integrator, and the input is I_{z-} where $I_{z-} = -kI_{o1}$. Thus, the relationship of I_{o1} and I_{o2} can be given by

$$I_{o2}=\frac{k_1}{k_2}\left(\frac{1}{sC_1R_{x2}}\right)I_{o1} \tag{21}$$

Thus, the phase difference between I_{o1} and I_{o2} is 90°, the phase difference between I_{o2} and I_{o3} is 180°, and the phase of I_{o2} leads the phase of I_{o1} for 90°. Therefore, the proposed current-mode quadrature oscillator provides three output currents with a phase shift of 90°.

It could be noted that output currents I_{o1}, I_{o2}, and I_{o3} are supplied from z-terminals of CCCII, so they have a high impedance level that can be fed to the load without the use of buffer circuits.

5. Simulation Results

SPICE simulations were performed to verify the characteristics of the proposed versatile filter in Figure 2. The CCCII in Figure 1 was performed with the transistor model parameters of AT&T's ALA400 CBIC-R process [43]. The DC supply voltage was ±2.5 V, and the capacitors C_1 and C_2 were 10 nF. The bias currents I_{set1} and I_{bi} were equal to 25 μA, and the bias current I_{ai} was used to control the current gain k_i (i = 1, 2). The summarized performance of the CCCII used in this paper is shown in Table 1. Figure 5 illustrates the magnitude (a) and phase (b) responses of the LP and HP filters when the bias current I_{set2} was given as 10 μA, and the bias currents I_{a1} and I_{a2} were given 25 μA. The simulated pole frequency was 12.8 kHz, and the power consumption was 2.72 mW, whereas the theoretical value of the pole frequency was 12.24 kHz. Thus, the percent error of simulated pole frequency was 1.96%. The high-frequency limitation of the filter is approximately 10 MHz, and the magnitude of filters such as HP and AP responses will be slowly decreased when the frequency is higher than appropriately 5 MHz.

Table 1. Summarized performances of used CCCII.

Parameters	Value
Supply voltage	±2.5 V
Technology	BJT (ALA400 CBIC-R)
DC voltage range	−1.7 V to 1.7 V
Voltage gain	0.999
Current gain:	
I_{z-}/I_x	1.01
I_{kz+}/I_x (k = 1)	1.02
−3 dB bandwidth VF	37.4 MHz
−3 dB bandwidth CF:	
I_{z-}/I_x	14.6 MHz
I_{kz+}/I_x (k = 1)	14.6 MHz
Power consumption ($I_{set} = I_a = I_b$ = 25 μA)	1.84 mW
R_x (I_b = 1–100 μA)	13.27 kΩ–0.134 kΩ
$R_y//C_y$	1.48 MΩ//5 pF
$R_{z-}//C_{z-}$	375 kΩ//6 pF
$R_{kz+}//C_{kz+}$	373.7 kΩ//4.2 pF

Figure 6 shows the magnitude and phase responses of the AP filters. Figure 6a shows the magnitude and phase responses of the non-inverting AP filter (phase lag) obtained by summing up I_{o2} and I_{o3}, and Figure 6b shows the magnitude and phase responses of the inverting AP filter (phase lead) obtained by summing up I_{o1} and I_{o4}. It is clear from Figures 5 and 6 that the proposed filter can provide both non-inverting and inverting transfer functions of LP, HP, and AP filters in the same topology.

The non-inverting AP filter has been used by applying the input frequency of 1 kHz and varying the amplitude to test the linearity of the proposed filter. The total harmonic distortion (THD) with different amplitudes of I_{in} is shown in Figure 7, which shows that the THD was 1% for the amplitude of 40 $\mu A_{p\text{-}p}$.

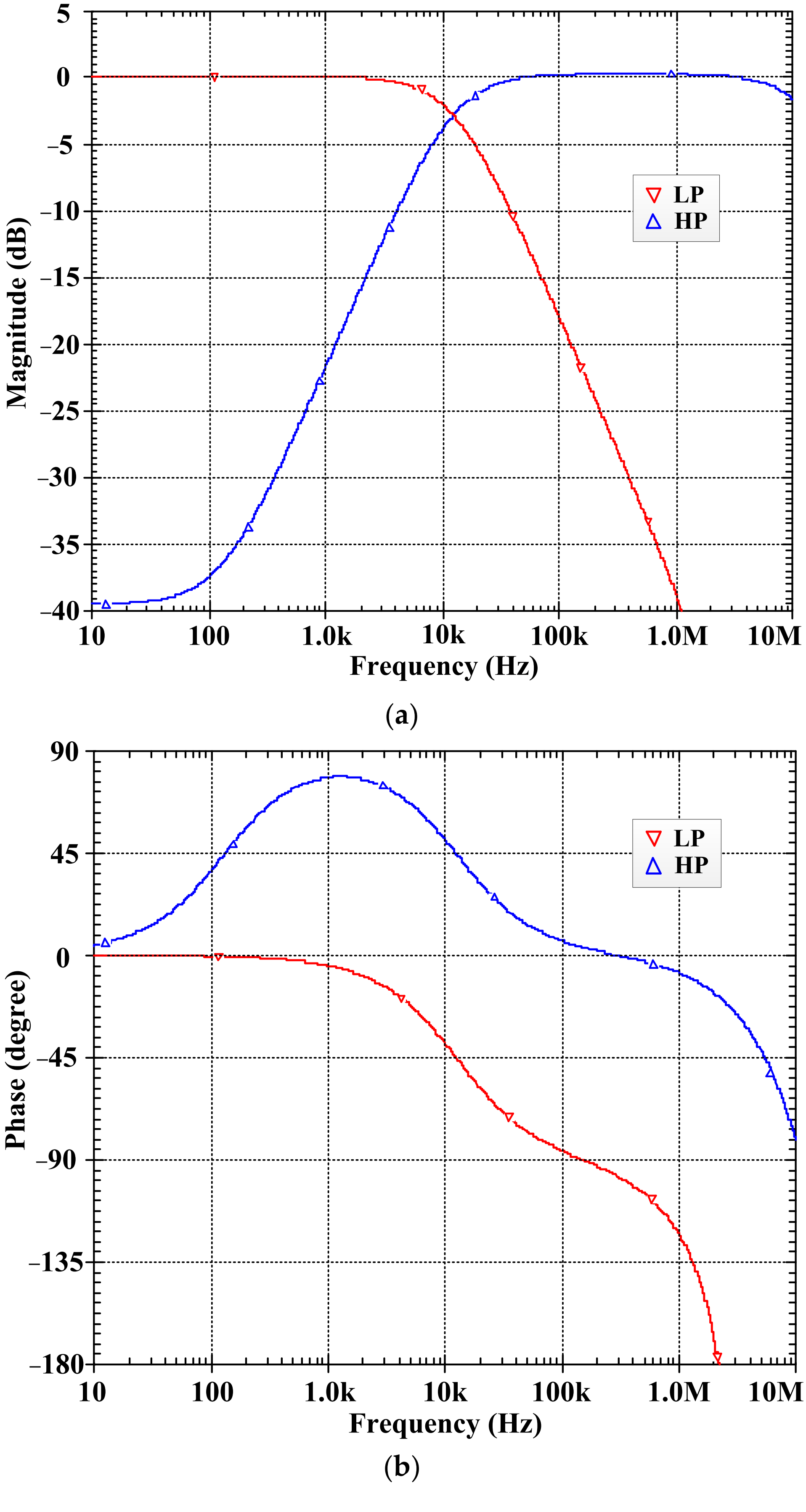

(**a**)

(**b**)

Figure 5. Frequency responses of LP and HP filters, (**a**) magnitude, (**b**) phase.

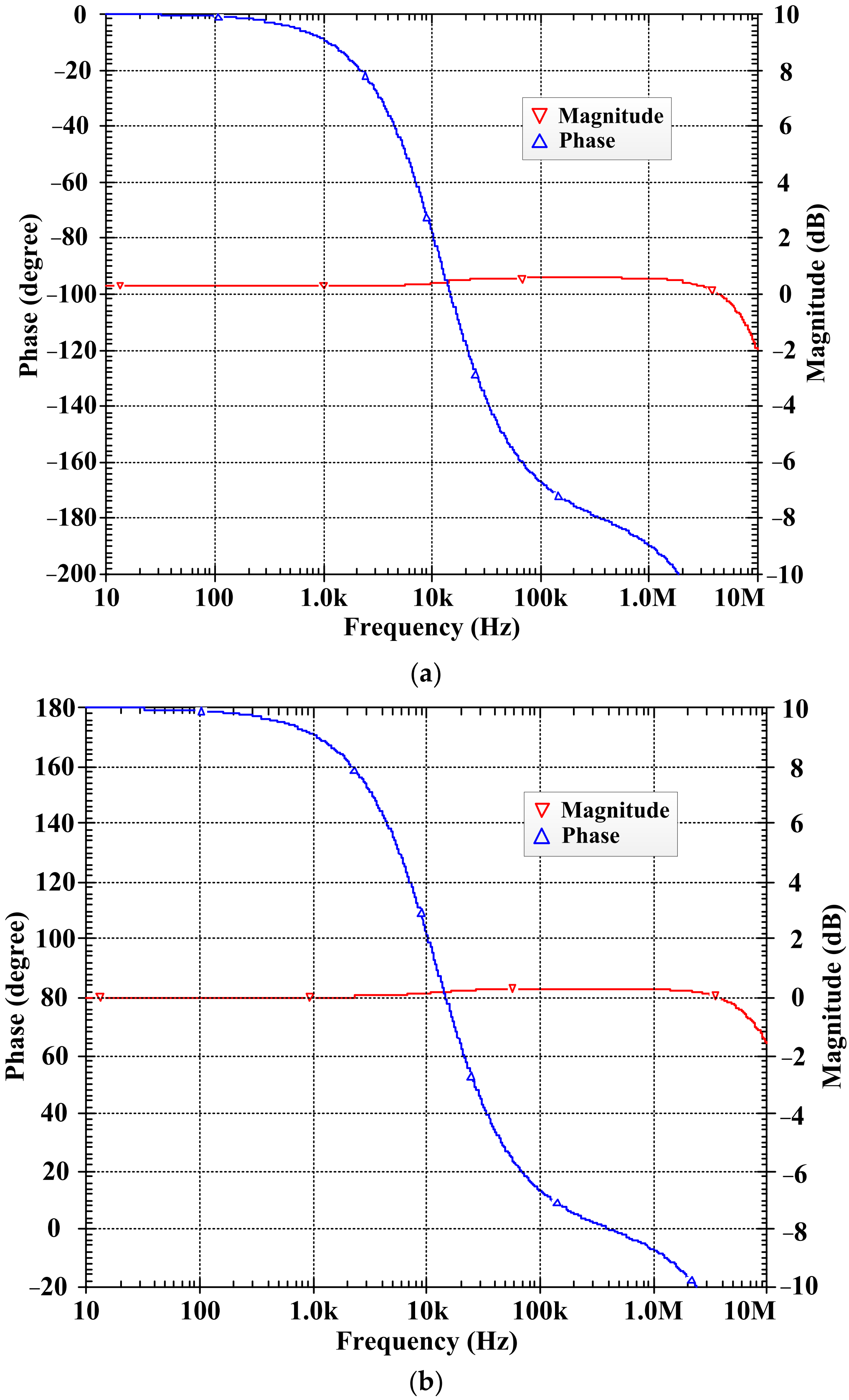

Figure 6. Magnitude and phase frequency responses of AP filters, (**a**) non-inverting (phase-lag), (**b**) inverting (phase-lead).

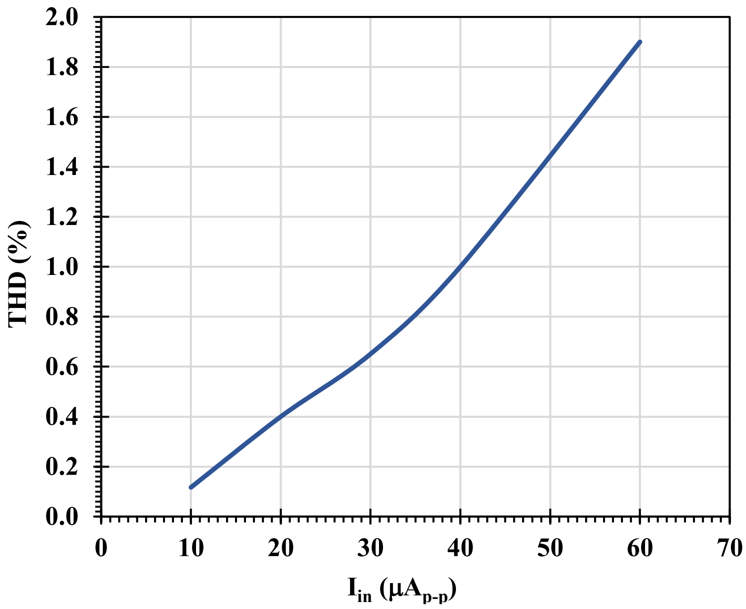

Figure 7. The THD with different amplitude of I_{in}.

Figure 8 showed the frequency responses when the pole frequency was varied by R_{x2} via the bias current I_{set2}. Figure 8a shows the variant magnitude frequency response of the LP filter, (b) variant magnitude frequency response of the HP filter, (c) variant phase frequency response of the non-inverting AP filter (phase-lag), (d) phase frequency response of the inverting AP filter (phase-lead), when the bias current I_{set2} was changed as 5 µA, 10 µA, 25 µA, 50 µA, and 100 µA and the obtaining pole frequency were, respectively, 6.33 kHz, 12.8 kHz, 31.13 kHz, 60.98 kHz, and 117.61 kHz. This result is used to confirm that the proposed filter can tune the pole frequency using the single bias current I_{set2} without matching conditions for other parameters.

Figure 9 shows the magnitude frequency responses for (a) LP filter, (b) HP filter, and (c) AP filter when the gains were varied by k_1 and/or k_2 via the bias currents I_{a1} and/or I_{a2} (I_{b1} and I_{b2} were set to 25 µA). The current gains were −0.36 dB, 0.3 dB, 6.1 dB, 9.6 dB, and 11.8 dB when the bias currents I_{a1} and/or I_{a2} were set to 15 µA (k = 0.6), 25 µA (k = 1), 50 µA (k = 2), 75 µA (k = 3), and 100 µA (k = 4), respectively.

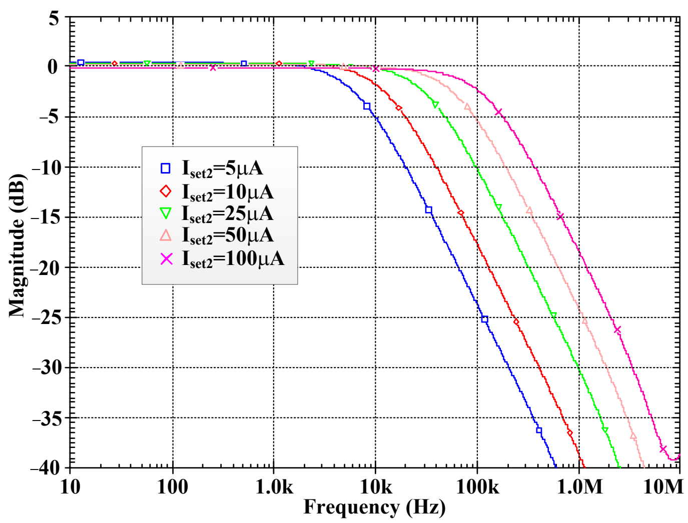

(**a**)

Figure 8. *Cont.*

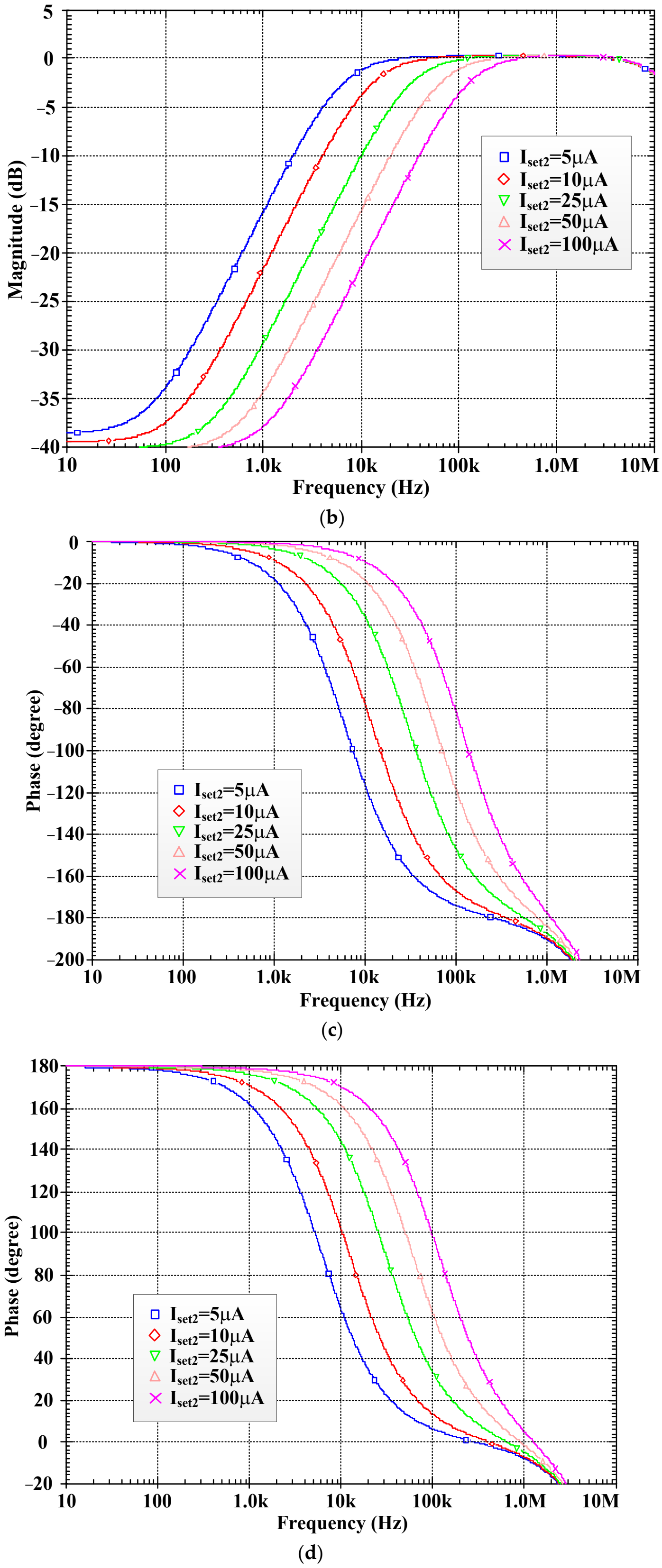

Figure 8. Magnitude and phase frequency responses when pole frequency is varied by I_{set2} for (**a**) LP filter, (**b**) HP filter, (**c**) non-inverting AP filter (phase-lag), (**d**) inverting AP filter (phase-lead).

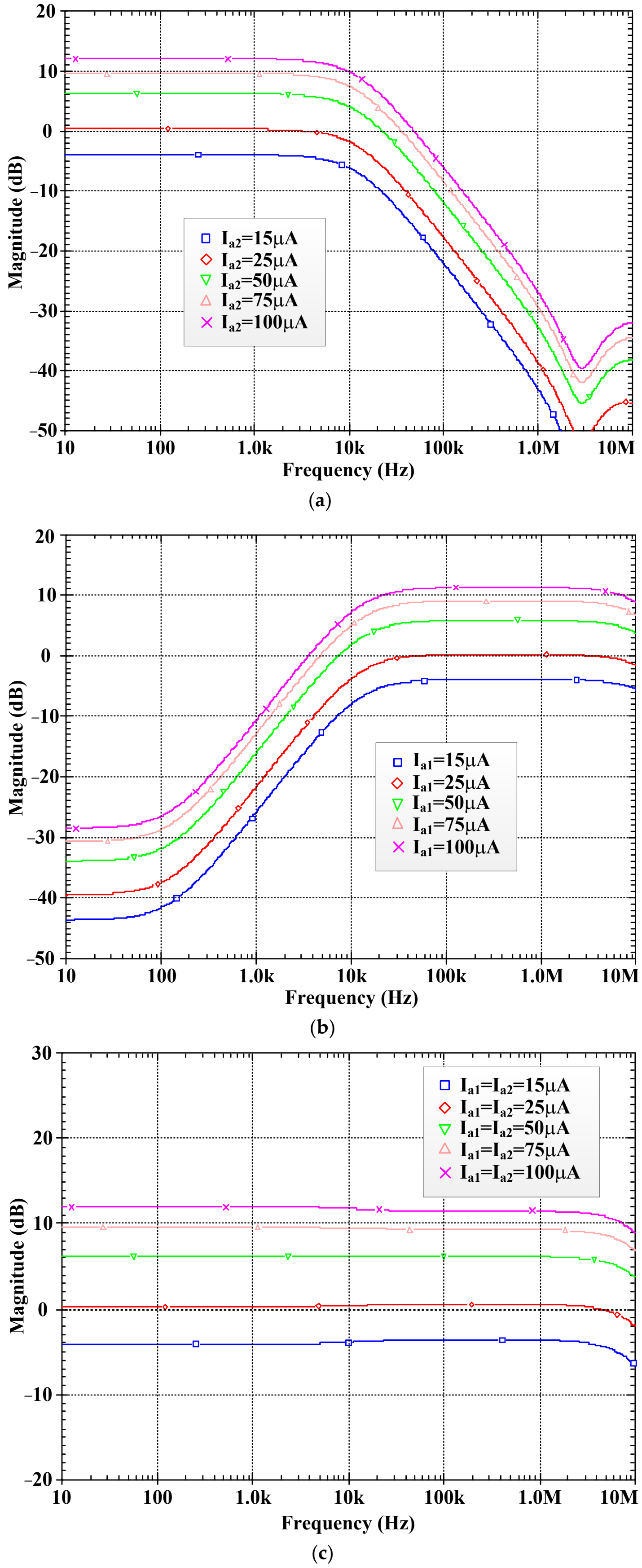

Figure 9. Magnitude frequency responses when magnitude is varied for (**a**) LP filter, (**b**) HP filter, (**c**) AP filter.

The simulated magnitude frequency responses of the LP, HP, and AP filters for process, voltage, and temperature (PVT) corners were investigated. Figures 10 and 11 show, respectively, the results of the Monte-Carlo (MC) analysis were variations of the beta (β) in BJT by 10% (LOT tolerance) and supply voltages by $\pm$10%. Figure 12 shows the magnitude frequency responses when the temperature was changed from -20 to 85 °C. It can be noted that the magnitude frequency responses were slightly changed when the process, voltage, and temperature were varied. From Figure 10, the maximum variations of passband gains of LP, HP, and AP filters were, respectively, about 0.07 dB, 0.15 dB, and 0.06 dB, while the maximum variations of the passband gains of LP, HP, and AP filters were respectively about 0.14 dB, 0.11 dB, and 0.19 dB for Figure 11, and the maximum variations of passband gains of LP, HP, and AP filters were, respectively, about 0.32 dB, 0.69 dB, 0.53 dB for Figure 12. Since temperature also affects the pole frequency via R_{x1} and R_{x2} (2), considering the temperatures of $-20°$ and $85°$, the pole frequencies were respectively 14.37 kHz and 11.14 kHz, which differed by 3.23 kHz.

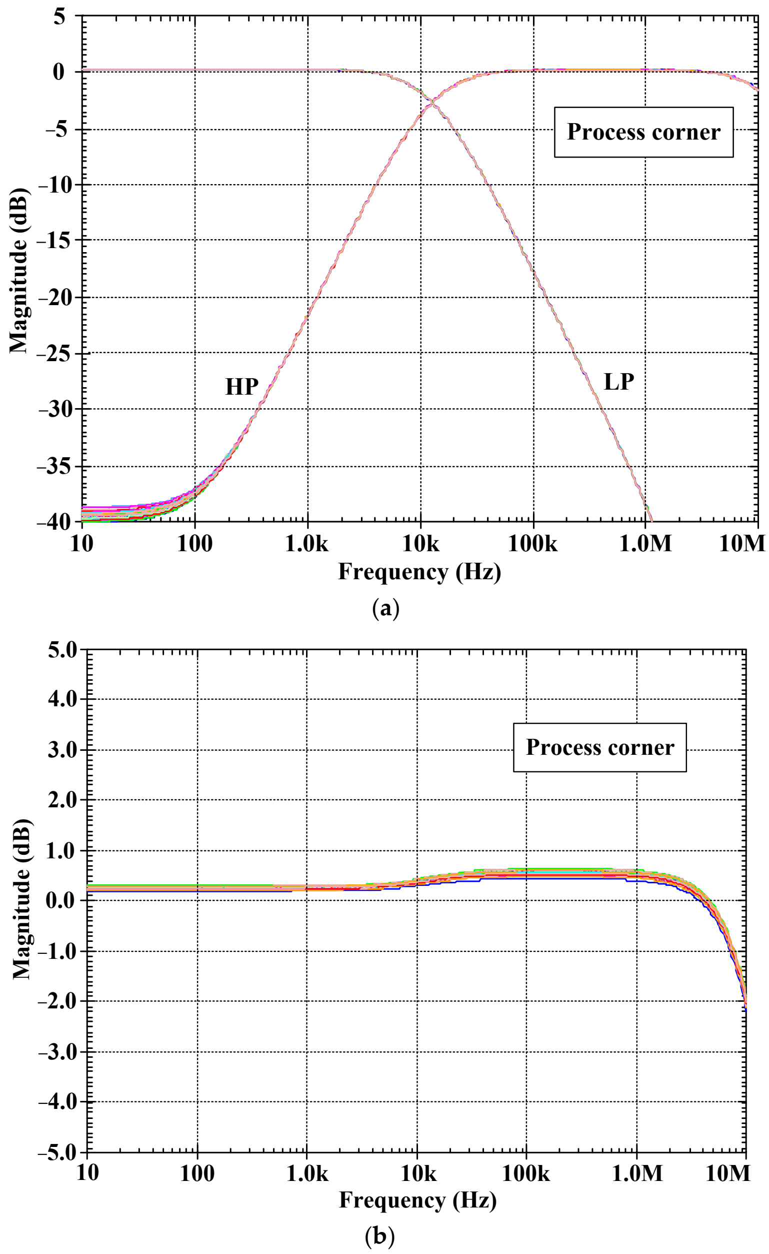

Figure 10. Magnitude frequency responses for process corner, (**a**) LP and HP filters, (**b**) AP filter.

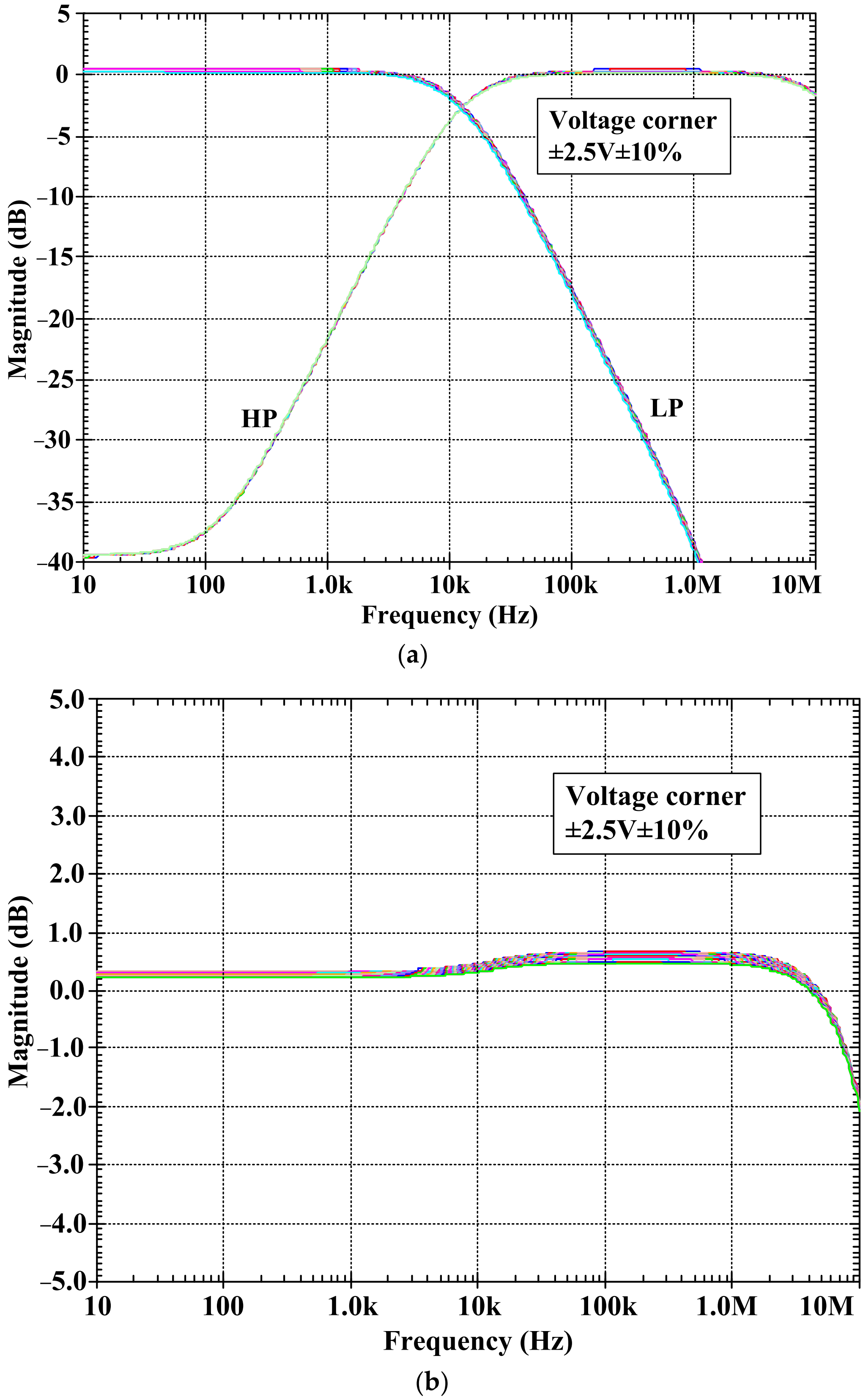

Figure 11. Magnitude frequency responses voltage corner, (**a**) LP and HP filters, (**b**) AP filter.

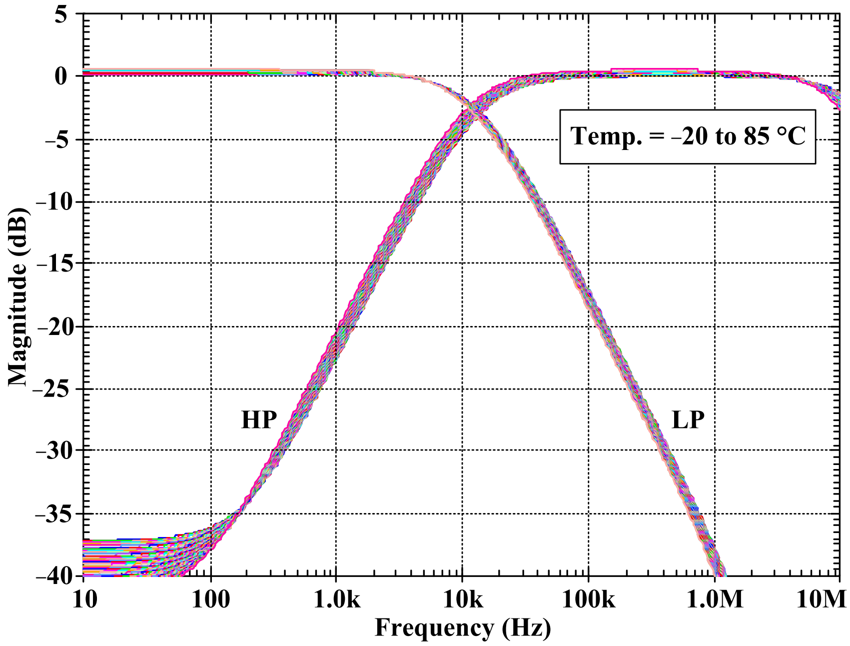

(**a**)

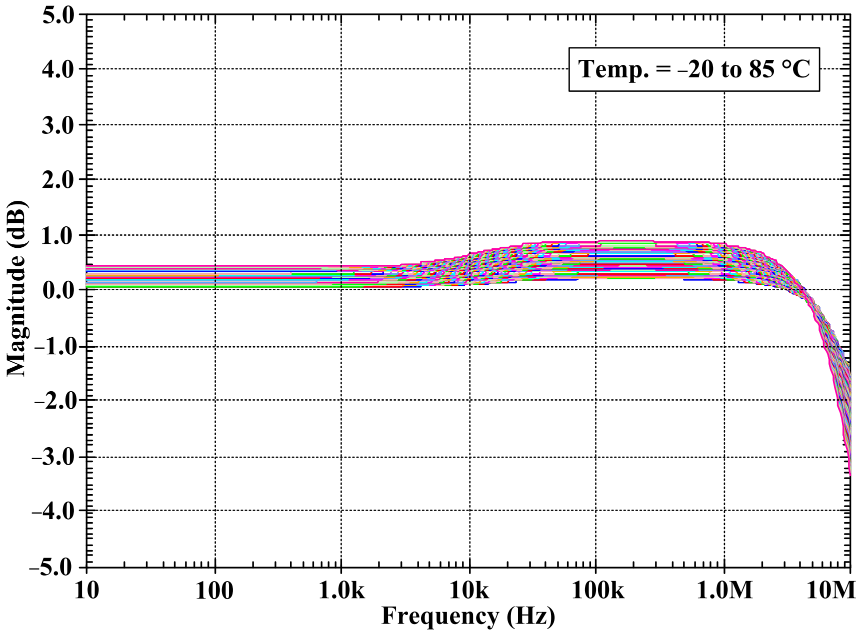

(**b**)

Figure 12. Magnitude frequency responses when temperature is varied from −20 to 85 °C, (**a**) LP, and HP filters, (**b**) AP filter.

The LP response was simulated by setting 5% tolerances of the capacitor C_1 at the pole frequency of 12.8 kHz and 200 Gaussian distribution runs. Figure 13 shows the derived histogram of the cut-off frequency, which expressed that the standard deviation (σ) of f_o was 0.631 kHz, and the maximum and minimum values of f_o were, respectively, 14.496 kHz and 11.518 kHz. It is worth noting that thanks to the electronic tunability of the filter, the deviation of the cut-off frequency and the gain could be easily readjusted by the I_{set2} and I_a, respectively.

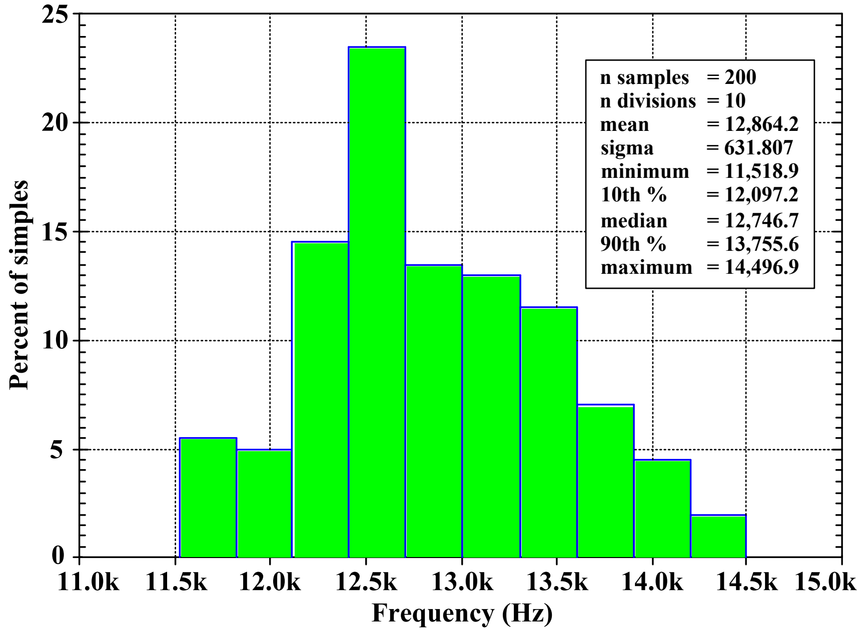

Figure 13. The histogram of the cut-off frequency of the LP filter with 200 runs of MC analysis.

The comparison of the proposed filter with the previous works is in Table 2. The VM first-order filter in [10], mixed-mode (MM) first-order filters [11,34], and CM first-order filters in [11,24,26,29] have been used to compare. Compared with [10,11,26,29], the proposed filter offers six transfer functions similar to [24], but for the filter in [24], the gain of the transfer functions cannot be controlled. The MM first-order filter in [34] offers VM, trans-admittance mode (TAM), CM, and trans-impedance mode (TIM) operation from the same circuit structure, but each operation mode provides only three transfer functions of LP, HP, and AP filters whereas the proposed filter offers six transfer functions of LP, HP, AP filters. Compared to [10,11,24,34], this realization uses only grounded capacitors and does not require a passive resistor. Finally, compared to [11,24,34], the proposed current-mode filter offers low-input and high-output impedances.

Table 2. Comparison with previous first-order filters.

Features	Proposed	[10] 2022	[11] 2021	[24] 2017	[26] 2019	[29] 2022	[34] 2023
Active and passive elements	2 CCCII, 2 C	1 LT1228, 2 R, 1 C	2 CVCII, 1 C, 2 R (Figure 2)	2 ICCII, 1 C, 1 MOS	1 DXCCTA, 2 C	1 MOCDTA, 1 C	1 VDGA, 1 C, 1 R
Realization	BJT process (ALA400 CBIC-R)	Commercial IC	CMOS structure (0.18 μm)	CMOS structure (0.13 μm)	CMOS structure (0.18 μm)	CMOS structure (0.13 μm)	CMOS structure (0.18 μm)
Mode operation	CM	VM	CM, TIM	CM	CM	CM	MM
Type of filter	SIMO	MISO	SIMO	SIMO	SIMO	MIMO	MIMO
Number of filtering functions	6 (LP+, LP-, HP+, HP-, AP+, AP-)	4 (LP+, HP+, AP+, AP-)	2 (LP+, AP+)	6 (LP+, LP-, HP+, HP-, AP+, AP-)	4 (LP-, HP+, AP-)	3 (LP+, HP+, AP+)	3 (LP-, HP+, AP-)

Table 2. *Cont.*

Features	Proposed	[10] 2022	[11] 2021	[24] 2017	[26] 2019	[29] 2022	[34] 2023
Electronic control of gain	Yes	LP+, HP+	Yes	No	No	No	Yes
Low-input and high-output impedance	Yes	-	No	No	Yes	Yes	No
Using grounded capacitor/resistor	Yes	No	No	No	Yes	Yes	No
Pole frequency (kHz)	12.3	90	89–1000	2600	10,000	1590	1590
Electronic control of parameter ω_o	Yes	Yes	Yes	Yes	Yes	Yes	Yes
Total harmonic distortion (%)	1@40 μA_{pp}	1@200 mV_{pp}	2@30 μA_{pp}	<1.5@90 μA_{pp}	-	-	-
Power supply voltages (V)	±2.5	±5	±0.9	±0.75	±1.25	±1	±0.9
Power consumption (mW)	2.72	57.6	1.057	4.08	1.75	2.5	1.31
Verification of result	Sim.	Exp.	Sim./Exp.	Sim.	Sim./Exp.	Sim./Exp.	Sim./Exp.

Note: MOCDTA = multiple-output current differencing transconductance amplifier, DXCCTA = dual-X current conveyor transconductance amplifier, VDGA = voltage differencing gain amplifier, CVCII = Electronically controllable second-generation voltage conveyors, TIM = trans-impedance mode, SIMO = single-input multiple-output, MISO = multiple-input single-output, MIMO = multiple-input multiple-output, MM = mixed-mode.

The current-mode quadrature oscillator in Figure 4 was simulated, and the CCCII with controlled current gain in Figure 1a was used. The bias current I_{b1} and I_{b2} of $CCCII_1$ and $CCCII_2$ were set to 25 µA, and the bias current I_{a1} of $CCCII_1$ was 36 µA for controlling the condition of oscillation. Figure 14 shows the simulated outputs of the oscillator when C_1 and C_2 were set to 10 nF, the bias current I_{set1} of $CCCII_1$ and the bias current I_{set3} of $CCCII_2$ were given as 25 µA, and the bias current I_{set2} of $CCCII_2$ was given as 10 µA. The oscillating frequency of 20.8 kHz was obtained, whereas the theoretical value of the oscillating frequency was 19.35 kHz. It could be noted that the amplitudes of output currents I_{o1}, I_{o2}, and I_{o3} were almost equal. In this case, the bias current I_{a2} of $CCCII_2$ of 50 µA was used to control the currents I_{o2} and I_{o3}. It can also be noted that when the condition of oscillation was varied by R_{x2} and R_{x3} and led to the difference of amplitudes of I_{o1} and I_{o2}, I_{o3}, the problem can be solved by adjusting k_2 of $CCCII_2$ via the bias current I_{a2} to achieve the same amplitudes. This option of tuning is available thanks to the advantage of the CCCII circuit with controlled gain.

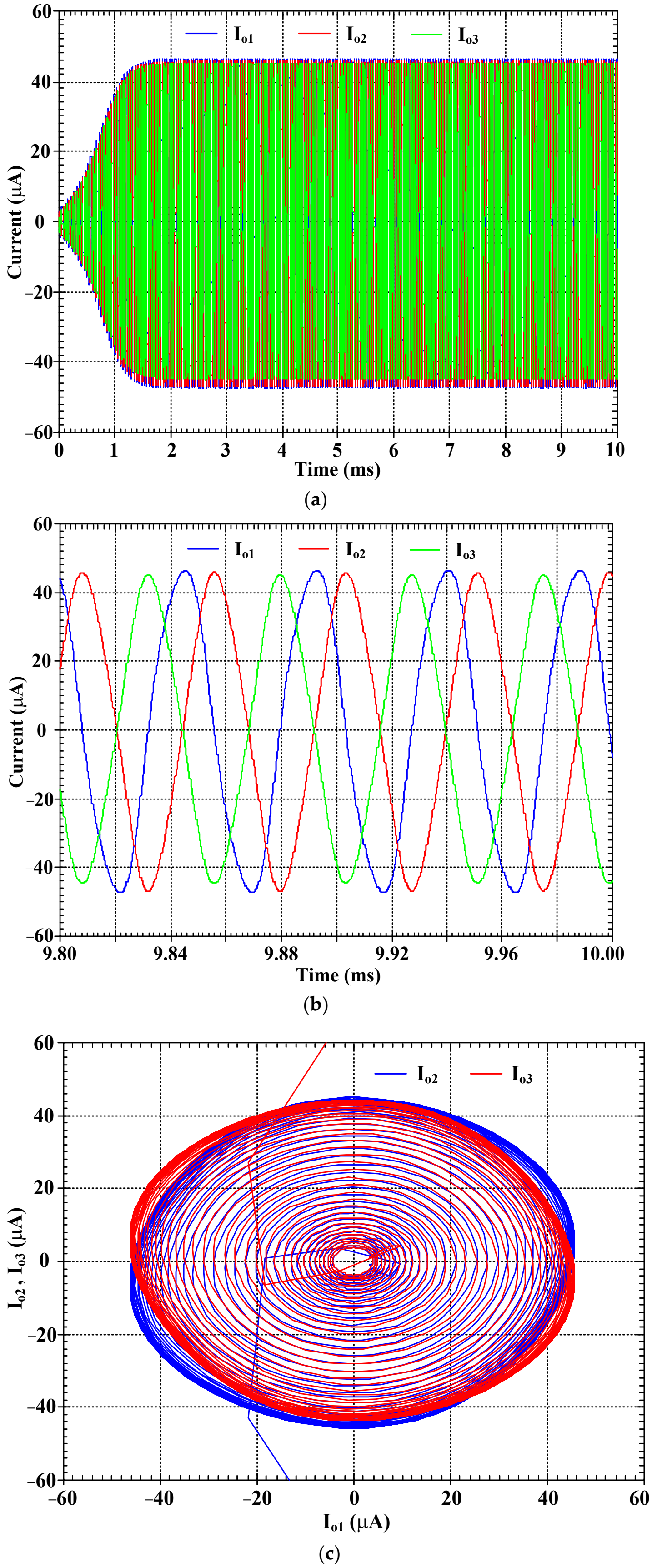

Figure 14. Simulated outputs of oscillator, (**a**) running oscillation, (**b**) steady state, (**c**) quadrature relationship between I_{o1} and I_{o2}, I_{o1}, and I_{o3}.

6. Conclusions

A new current-mode first-order versatile filter using two translinear current conveyors with controlled current gain and one grounded capacitor is presented in this paper. The proposed filter offers the following features: (1) realizations of non-inverting and inverting transfer functions of low-pass, high-pass, and all-pass filters into single topology, (2) control of the current gain for all transfer functions of the filters, (3) electronic control of a pole frequency, (4) no requirement of component-matching conditions for realizing all filter responses, (5) low-input impedance and high-output impedance. The proposed first-order filter has been applied to realize the current-mode quadrature sinusoidal oscillator. The proposed filter and its application were simulated with SPICE to confirm characteristics and workability.

Author Contributions: Conceptualization, M.K. and N.W.; methodology, M.K., F.K. and T.K.; software, M.K., P.P. and F.K.; validation, W.J., P.P. and F.K.; investigation, W.J.; resources, N.W.; writing—original draft, M.K., W.J., N.W., P.P., F.K. and T.K.; supervision, F.K. All authors have read and agreed to the published version of the manuscript.

Funding: This work was supported in part by the University of Defence within the Organization Development Project VAROPS.

Data Availability Statement: Not applicable.

Conflicts of Interest: The authors declare no conflict of interest.

References

1. Roberts, G.; Sedra, A. All current-mode frequency selective circuits. *Electron. Lett.* **1989**, *25*, 759–761. [CrossRef]
2. Toumazou, C.; Lidgey, F.J.; Haig, D.G. *Analogue IC Design: The Current-Mode Approach*; Peter Peregrinus: London, UK, 1990.
3. Toker, A.; Ozoguz, S.; Cicekoglu, O.; Acar, C. Current-mode all-pass filters using current differencing buffered amplifier and a new high-Q bandpass filter configuration. *IEEE Trans. Circuits Syst. II Analog. Digit. Signal Process.* **2000**, *47*, 949–954. [CrossRef] [PubMed]
4. Gift, S.J.G. The application of all-pass filters in the design of multiphase sinusoidal systems. *Microelectron. J.* **2000**, *31*, 9–13. [CrossRef]
5. Idros, M.F.B.M.; Abu Hassan, S.F.B. A design of butterworth low pass filter's layout basideal filter approximation on the ideal filter approximation. In Proceedings of the 2009 IEEE Symposium on Industrial Electronics & Applications, Kuala Lumpur, Malaysia, 4–6 October 2009; pp. 754–757. [CrossRef]
6. Kumari, S.; Nand, D. DDCC-based MISO type voltage-mode first-order universal filter. In Proceedings of the 2022 2nd International Conference on Intelligent Technologies (CONIT), Hubli, India, 24–26 June 2022; pp. 1–6. [CrossRef]
7. Dogan, M.; Yuce, E. A first-order universal filter including a grounded capacitor and two CFOAs. *Analog. Integr. Circuits Signal Process.* **2022**, *112*, 379–390. [CrossRef]
8. Singh, P.; Varshney, V.; Kumar, A.; Nagaria, R. Electronically tun-able first order universal filter based on CCDDCCTA. In Proceedings of the 2019 IEEE Conference on Information and Communication Technology, Allahabad, India, 6–8 December 2019; pp. 1–6. [CrossRef]
9. Jaikla, W.; Talabthong, P.; Siripongdee, S.; Supavarasuwat, P.; Suwanjan, P.; Chaichana, A. Electronically controlled voltage mode first order multifunction filter using low-voltage low-power bulk-driven OTAs. *Microelectron. J.* **2019**, *91*, 22–35. [CrossRef]
10. Jaikla, W.; Buakhong, U.; Siripongdee, S.; Khateb, F.; Sotner, R.; Silapan, P.; Suwanjan, P.; Chaichana, A. Single Commercially Available IC-Based Electronically Controllable Voltage-Mode First-Order Multifunction Filter with Complete Standard Functions and Low Output Impedance. *Sensors* **2021**, *21*, 7376. [CrossRef]
11. Barile, G.; Safari, L.; Pantoli, L.; Stornelli, V.; Ferri, G. Electronically Tunable First Order AP/LP and LP/HP Filter Topologies Using Electronically Controllable Second Generation Voltage Conveyor (CVCII). *Electronics* **2021**, *10*, 822. [CrossRef]
12. Duangmalai, D.; Suwanjan, P. The voltage-mode first order universal filter using single voltage differencing differential input buffered amplifier with electronic controllability. *Int. J. Electr. Comput. Eng. IJECE* **2022**, *12*, 1308–1323. [CrossRef]
13. Singh, P.; Nagaria, R.K. Voltage mode and trans-admittance mode first-order universal filters employing DV-EXCCCII. *Aust. J. Electr. Electron. Eng.* **2022**, *19*, 396–406. [CrossRef]
14. Dogan, M.; Yuce, E.; Dicle, Z. CFOA-based first-order voltage-mode universal filters. *AEU Int. J. Electron. Commun.* **2023**, *161*. [CrossRef]
15. Li, Y.-A. A series of new circuits based on CFTAs. *AEU Int. J. Electron. Commun.* **2012**, *66*, 587–592. [CrossRef]
16. Herencsar, N.; Lahiri, A.; Koton, J.; Vrba, K. First-order multifunction filter design using current amplifiers. In Proceedings of the 2016 39th International Conference on Telecommunications and Signal Processing (TSP), Vienna, Austria, 27–29 June 2016; pp. 279–282. [CrossRef]

17. Kumar, A.; Paul, S.K. Current mode first order universal filter and multiphase sinusoidal oscillator. *AEU Int. J. Electron. Commun.* **2017**, *81*, 37–49. [CrossRef]
18. Chaturvedi, B.; Mohan, J.; Jitender; Kumar, A. A novel realization of current-mode first order universal filter. In Proceedings of the 2019 6th International Conference on Signal Processing and Integrated Networks (SPIN), Noida, India, 7–8 March 2019; pp. 623–627. [CrossRef]
19. Horng, J.-W.; Wu, C.-M.; Zheng, J.-H.; Li, S.-Y. Current-mode first-order highpass, lowpass, and allpass filters using two ICCIIs. In Proceedings of the 2020 IEEE International Conference on Consumer Electronics-Taiwan (IC-CE-Taiwan), Taoyuan, Taiwan, 28–30 September 2020; pp. 1–2. [CrossRef]
20. Yucel, F. A DVCC-Based Current-Mode First-Order Universal Filter. *J. Circuits Syst. Comput.* **2021**, *30*, 2150305. [CrossRef]
21. Yuce, E.; Minaei, S. A new first-order universal filter consisting of two ICCII + s and a grounded capacitor. *AEU Int. J. Electron. Commun.* **2021**, *137*, 153802. [CrossRef]
22. Raj, A.; Bhaskar, D.R.; Senani, R.; Kumar, P. Extension of recently proposed two-CFOA-GC all pass filters to the realisation of first order universal active filters. *AEU Int. J. Electron. Commun.* **2022**, *146*, 154119. [CrossRef]
23. Herencsar, N.; Koton, J.; Sagbas, M.; Ayten, U.E. New tunable resistorless CM first-order filter based on single CBTA and grounded capacitor. In Proceedings of the 2016 IEEE 59th International Midwest Symposium on Circuits and Systems (MWSCAS), Abu Dhabi, United Arab Emirates, 16–19 October 2016; pp. 1–4. [CrossRef]
24. Safari, L.; Yuce, E.; Minaei, S. A new ICCII based resistor-less current-mode first-order universal filter with electronic tuning capability. *Microelectron. J.* **2017**, *67*, 101–110. [CrossRef]
25. Agrawal, D.; Maheshwari, S. An Active-C Current-Mode Universal First-Order Filter and Oscillator. *J. Circuits Syst. Comput.* **2019**, *28*, 1950219. [CrossRef]
26. Chaturvedi, B.; Kumar, A.; Mohan, J. Low Voltage Operated Current-Mode First-Order Universal Filter and Sinusoidal Oscillator Suitable for Signal Processing Applications. *AEU Int. J. Electron. Commun.* **2019**, *99*, 110–118. [CrossRef]
27. Chaturvedi, B.; Mohan, J.; Jitender; Kumar, A. Resistorless Realization of First-Order Current Mode Universal Filter. *Radio Sci.* **2020**, *55*, e2019RS006932. [CrossRef]
28. Mohan, J.; Chaturvedi, B.; Jitender. CMOS Compatible First-Order Current Mode Universal Filter Structure and its Possible Tunable Variant. *J. Circuits Syst. Comput.* **2022**, *31*, 2250242. [CrossRef]
29. Kumar, A.; Kumar, S.; Elkamchouchi, D.H.; Urooj, S. Fully Differential Current-Mode Configuration for the Realization of First-Order Filters with Ease of Cascadability. *Electronics* **2022**, *11*, 2072. [CrossRef]
30. Chaturvedi, B.; Kumar, A. Electronically Tunable First-Order Filters and Dual-Mode Multiphase Oscillator. *Circuits Syst. Signal Process.* **2019**, *38*, 2–25. [CrossRef]
31. Rohilla, K.; Pushkar, K.L.; Kumar, R.; Raj, A. Resistorless First-Order Universal Filter Structures Employing OTAs with Independent Controllability of Gain and Pole Frequency. *IETE J. Res.* **2022**. [CrossRef]
32. Raj, A. Mixed-Mode Electronically-Tunable First-Order Universal Filter Structure Employing Operational Transconductance Amplifiers. *J. Circuits Syst. Comput.* **2022**, *31*, 2250234. [CrossRef]
33. Bhaskar, D.R.; Raj, A.; Senani, R.; Kumar, P. CFOA-based simple mixed-mode first-order universal filter configurations. *Int. J. Circuit Theory Appl.* **2022**, *50*, 2631–2641. [CrossRef]
34. Roongmuanpha, N.; Likhitkitwoerakul, N.; Fukuhara, M.; Tangsrirat, W. Single VDGA-Based Mixed-Mode Electronically Tunable First-Order Universal Filter. *Sensors* **2023**, *23*, 2759. [CrossRef]
35. Fabre, A.; Saaid, O.; Wiest, F.; Boucheron, C. Current controlled bandpass filter based on translinear conveyors. *Electron. Lett.* **1995**, *31*, 1727–1728. [CrossRef]
36. Fabre, A.; Mimeche, N. Class A/AB second-generation current conveyor with controlled current gain. *Electron. Lett.* **1994**, *30*, 1267–1269. [CrossRef]
37. Kumngern, M.; Jongchanachavawat, W.; Dejhan, K. New electronically tunable current-mode universal biquad filter using translinear current conveyors. *Int. J. Electron.* **2010**, *97*, 511–523. [CrossRef]
38. Kumngern, M.; Chanwutitum, J.; Dejhan, K. Electronically tunable multiphase sinusoidal oscillator using translinear current conveyors. *Analog. Integr. Circuits Signal Process.* **2010**, *65*, 327–334. [CrossRef]
39. Surakampontorn, W.; Kumwachara, K. Cmos-based electronically tunable current conveyor. *Electron. Lett.* **1992**, *28*, 1316–1317. [CrossRef]
40. Mimaei, S.; Sayin, O.K.; Kuntman, H. A New CMOS electronically tunable current conveyor and its application to current-mode filters. *IEEE Trans. Circuits Syst. I Regul. Pap.* **2006**, *53*, 1448–1458. [CrossRef]
41. Kumngern, M. A new CMOS second generation current conveyor with variable current gain. In Proceedings of the 2012 IEEE International Conference on Circuits and Systems (ICCAS), Kuala Lumpur, Malaysia, 3–4 October 2012; pp. 272–275. [CrossRef]
42. Abuelmaatti, M.; Al-Qahtani, M. A new current-controlled multiphase sinusoidal oscillator using translinear current conveyors. *IEEE Trans. Circuits Syst. II Analog. Digit. Signal Process.* **1998**, *45*, 881–885. [CrossRef]
43. Frey, D. Log-domain filtering: An approach to current-mode filtering. *IEE Proc. G Circuits Devices Syst.* **1993**, *140*, 406–416. [CrossRef]